IEEE International Electric Machines & Drives Conference

Miami, FL - May 21-24, 2017

Conference Program

IEEE PES Power & Energy Society®

pels IEEE POWER ELECTRONICS SOCIETY Powering a Sustainable Future

IAS IEEE INDUSTRY APPLICATIONS SOCIETY Linking Research to Practice

ICS

ENERGY SYSTEMS RESEARCH LABORATORY

Consideration of the manufacturing influence in standardized material characterizations using machine measurements

Silas Elfgen[1], Andreas Ruf[1], Simon Steentjes[1], Kay Hameyer[1]
[1]Institute of Electrical Machines, RWTH Aachen University, Aachen, Germany

Abstract— **Iron losses have a significant contribution to the overall losses of high power density electrical machines operating as variable speed drives. During production, mechanical stress is applied to the soft magnetic material resulting in local magnetic deterioration and hence rising iron losses. Dependent on the cutting technique, geometrical sizes of tooth and yoke width or external loads from housing and shaft, the resulting local iron losses increase significantly. Hence, standardized Epstein or single sheet measurements under ideal sinusoidal condition underestimate the resulting machine's iron losses as the geometrical specimen sizes are to large to quantify the manufacturing influences. This paper applies a semi-physical approach to test bench machine measurements. The approach is derived from the parameter identification of an iron loss formula in due consideration of the different frequency and flux density dependencies of the various iron loss components. Thereby, a calibration of the used iron loss formulation considering manufacturing influences is presented. This allows an a-priori assessment of realistic iron losses during the design stage.**

Keywords— manufacturing influences, iron losses, cut edge effects

I. INTRODUCTION

In today's high power density electrical machines iron losses take a significant share in the overall losses due to high magnetic utilization and high fundamental frequencies. In view of loss minimizing control strategies and thermal machine designs for PMSMs iron losses have to be taken into consideration due to the rising share across the operating map [1–3]. An accurate iron loss calculation is a crucial aspect, in order to find the corresponding direct and quadrature current that minimizes the total losses. The identification of loss parameters for present-day loss models is achieved in standardized measurements under ideal conditions. Standardized measurements using the *Epstein frame* (*EF*) or the *Single Sheet Tester* (*SST*) under sinusoidal flux density are reasonable in terms of a phenomenological comparison of different steel sheets or if single effects are to be compared e.g. by loss separation. But if the aim is a final machine design, the resulting losses must be known especially in view of a thermal design. In addition to the occurring flux densities and fundamental frequencies, the manufacturing process strongly influences the magnetic properties [4–7]. It is well known that soft magnetic materials are prone to mechanical stress. Especially in case of small machines designs, local material properties are adversely affected by residual cutting stress and housing [8, 9]. To identify the resulting magnetic loss parameters more accurately, the actual physical dimensions of the machine laminations along with the manufacturing aspects must be considered. This paper uses a semi-physical approach to identify machine iron loss parameters by using test bench measurements [10]. The results are compared to standard measurements, in order to demonstrate the influence of manufacturing on the resulting iron losses. The result is an a-priori assessment of manufacturing influences during the early design stage. For a physically accurate calculation of the resulting local flux density and loss distributions a local material model is necessary which allows one to represent the spatial variation of the magnetic properties [11].

The paper is structured as follows. First, an introduction to the model, which is used to calculate the resulting losses is given. Along with this sample preparation an identification of the according loss parameters is discussed. The measured machine is introduced followed by the identification of cut-edge-affected iron loss parameters. Compensation factors are introduced based on machine measurements to consider the manufacturing influence on the resulting iron losses. These are compared to the loss parameters that are identified on a standard measuring frame. Finally, a discussion and a brief summary is given.

II. METHODOLOGY

A. Iron Loss Model

The calculation of the resulting specific iron loss is conducted under standardized conditions using a SST [12, 12]. In order to identify the different loss contributions from measured data, the iron loss model presented in [13] is used. It is based on a semi-physical approach to identify the different loss model parameters from standardize EF or SST measurements. The iron loss model in (1) considers the contributions of static hysteresis P_{hyst}, eddy currents P_{cl}, excess P_{exc} and saturation losses P_{sat}. This approach is transferred to machine measurements of a permanent magnet synchronous (PMSM) machine with buried magnets. By introducing the saturation losses, the presented mathematical description copes with rising iron losses at rising frequencies f and by higher order terms of the magnetic flux density B:

978-1-5090-4281-4/17/$31.00 ©2017 IEEE

$$P_{\mathrm{Fe}} = P_{\mathrm{hyst}} + P_{\mathrm{cl}} + P_{\mathrm{exc}} + P_{\mathrm{sat}} \tag{1}$$

The loss contributions are calculated according to (2)-(5).

$$P_{\mathrm{hyst}} = a_1 \left(1 + \frac{B_{\mathrm{min}}}{B_{\mathrm{max}}} \left(r_{\mathrm{hyst}} - 1 \right) \right) B_{\mathrm{max}}^{\alpha} f_1 \tag{2}$$

$$P_{\mathrm{cl}} = a_2 \sum_{n=1}^{\infty} \left(B_n^2 \, (nf)^2 \right) \tag{3}$$

$$P_{\mathrm{exc}} = a_2 \sum_{n=1}^{\infty} \left(B_n^{1.5} \, (nf)^{1.5} \right) \tag{4}$$

$$P_{\mathrm{sat}} = a_2 a_3 B_{\mathrm{max}}^{a_4+2} f_1^2 \tag{5}$$

The hysteresis loss contribution in (2) takes the flux density loci in each element of the *finite element* (FE) model into account, by considering the minimum B_{min} and maximum B_{max} value of an electrical period along with a rotational loss factor r_{hyst} to consider rotational magnetization [14]. Parameter a_1 and α describe the hysteresis losses identified by DC-measurements using the SST under standardized conditions.

The classical loss parameter a_2 in (3) is identified according to Foucault eddy current losses in (6), using the analytical macroscopic equation depending on the thickness of the steel sheet d, the material density ρ and the electrical resistivity ρ_{el} of the electrical steel sheet.

$$a_2 = \frac{\pi^2 d^2}{6 \cdot \rho \rho_{el}} \tag{6}$$

The excess-loss contribution in (4) and excess-loss parameter a_5 is identified in the section of linear magnetization or at intermediate induction levels and at low frequencies where no skin effect appears. In this paper a measuring frequency of 10 Hz and polarizations up to 1.4 T are used for the identification of a_5. The empirical excess-loss factor can also be calculated according to [15] in terms of active magnetic objects and the domain wall motion leading to (7), with S the cross section of the steel lamination, $G \approx 0.136$ a dimensionless coefficient of the eddy-current damping and σ_{el}, the electrical conductivity of the lamination. Parameter V_0 attributes the local coercive fields and grain sizes [16].

$$a_5 = \sqrt{S V_0 \sigma_{\mathrm{el}} G} \tag{7}$$

Parameter a_3 and a_4 describe saturation losses of the material at higher frequencies and induction levels. They are mathematically fitted to measurement results

Classical and excess loss contributions in (3) and (4) respectively, are extended by a Fourier transformation of the local flux density in each finite element. The losses are calculated by adding up the harmonics of the flux density B_n, scaled by the corresponding frequency. Hysteresis, eddy and excess loss parameters are identified using the statistical loss theory [17] while saturation losses are mathematically fitted to measurements. Iron loss calculations are carried out considering higher harmonics n of the local flux density.

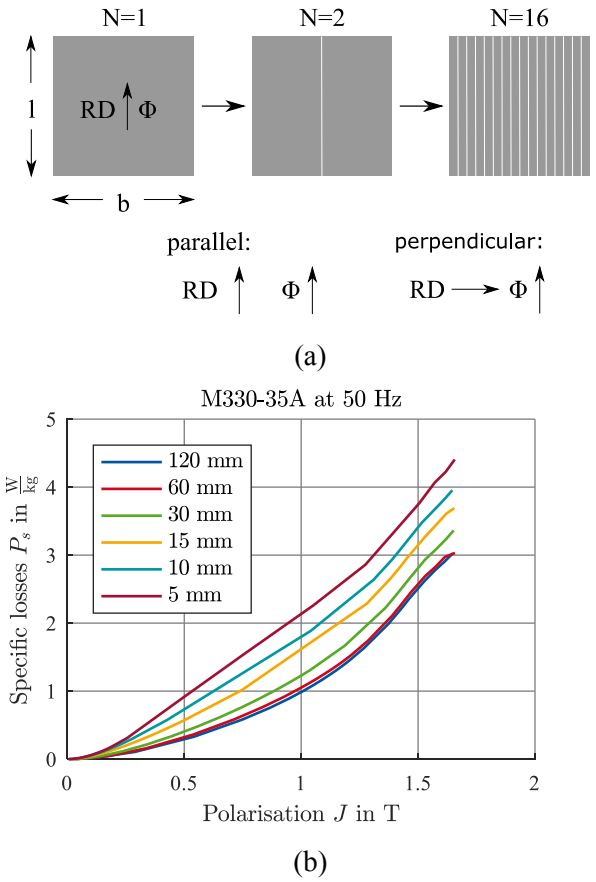

Fig. 1 (a) Sample preparation for single sheet measurements of different strip width ***b*** to consider cut edge effects due to manufacturing in iron loss measurements and (b) specific iron losses at 50 Hz of the different specimen width.

B. Iron loss parameter identification

Standardized measurement frames use specimen sizes of 30 mm and 120 mm width for EF and SST respectively. As the manufacturing influence on the magnetic properties of the lamination gets more pronounced at smaller strip width or a higher ratio of total cutting length to the volume, standardized specimen widths underestimate the resulting specific iron losses in rotating electrical machines. To consider the manufacturing influences on the resulting magnetization and iron loss behavior, material samples of different sizes according to the application's geometry must be characterized.

Consistently, single-sheet specimens of different strip width are laser cut per machine dimensions. As demonstrated in Fig. 1 (a) starting from a square of 120 mm x 120 mm (l x b) specimens are consecutively cut to smaller strip width while equaling a width of 120 mm in total. Specimens of both cases are considered. They are rolling direction (RD) and measured Flux Φ in parallel as well as, RD and measured Flux perpendicular to each other.

The machine under test is a synchronous machine with V-shaped buried permanent magnets (IPMSM) presented in [18]. The tooth and yoke width are 6 mm and 20 mm, respectively and significantly smaller when compared to standardized SST

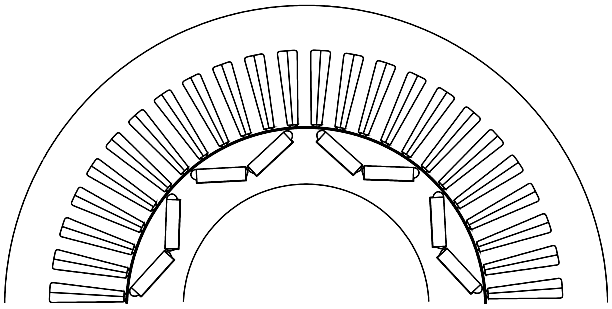

Fig. 2 Cross-section of used PMSM with burried permanent magnets.

TABLE I. SIMULATION AND MACHINE PARAMETER OF THE IPMSM

Magnet material	NdFeB
Number of Poles/Slots $2p/N$	8/48
Winding configuration	Distributed winding
Stator outer radius $r_{\mathrm{stator,o}}$	135 mm
Stator yoke width w_{st}	20 mm
Stator tooth width $w_{\mathrm{s,t}}$	6 mm
Rotor outer radius $r_{\mathrm{rotor,o}}$	80 mm
Rotor width w_{r}	25 mm
Axial length l_{Fe}	90 mm
Air gap length δ	0.7 mm
Battery voltage U_{dc}	400 V
Rated current I_{n}	142 A
Rated Torque M_n	162 Nm
Rated speed n_{n}	2500 min-1
Rated power P_{n}	42.4 kW

specimen widths. As demonstrated in Fig. 1 (b) the local magnetic properties and the resulting measured specific iron losses are considerably influenced by residual cutting stress with a decreasing strip width b [4, 6, 11].

The iron loss parameter identification is carried out on the SST measurement data and the loss parameters are identified as discussed before. With decreasing strip width, the relative share of local residual cutting stress increases. Consistently, both hysteresis loss parameter a_1 and α and excess loss parameter a_5 increases with smaller specimen width, as demonstrated in Fig**. 3** (a). Eddy loss parameter a_2 is considered to be constant as the parameters are not affected by the residual stress. Saturation losses are also influenced in terms of manufacturing, but do not result in an analytically describable distribution depending on the strip width.

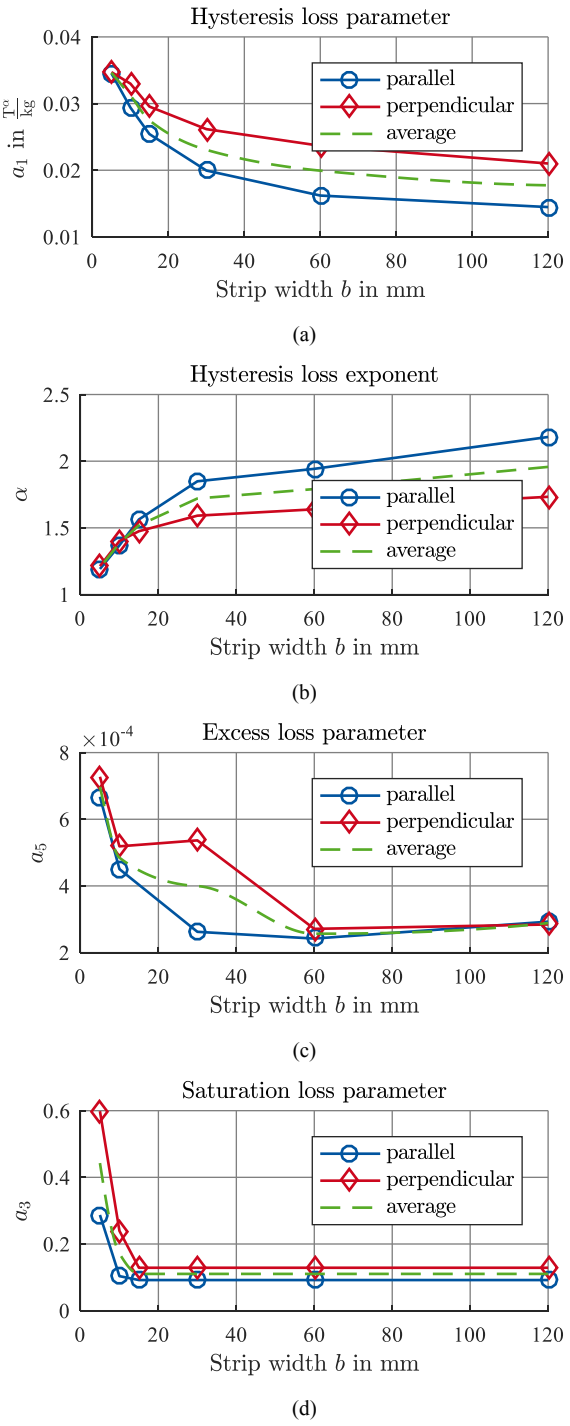

Fig. 3 (a),(b) Hysteresis loss parameter $\boldsymbol{a_1}$ and α, (c) excess loss parameter $\boldsymbol{a_5}$ and (d) saturation loss parameter $\boldsymbol{a_4}$ depending on the specimen strip width b.

In order to transfer the loss parameters from standardized material characterizations to a machine design, the actual dimensions of the machine core have to be taken into account. This allows one to cope with the influence of increased iron losses due to local magnetic material deterioration [11]. In case of hysteresis and excess losses, the deterioration increases proportional to the cutting length divided by the volume of the sliced material [11]. Using this approach, an a-priori estimation of the resulting iron loss parameter can be derived by scaling the

volume of the different sections e.g. stator tooth and stator yoke with the according cutting length as listed in TABLE I. Thereby the adapted iron loss parameter listed in TABLE II result.

C. Loss Parameter from test bench

To obtain an optimal set of iron loss parameters, machine test bench measurement are carried out at different speed values. At each speed level, overall machine losses are measured across the whole area of direct and quadrature current i_d, i_q. During measurements, the machine temperature is controlled to cope with changing copper losses. From the measured total losses P_Tot, copper P_Cu and friction losses P_Fr are subtracted to receive the measured total iron losses P_Fe. According to (1) the iron losses are separated into the different loss contributions which are identified using standardized measurements. To cope with manufacturing influences on the local magnetization behavior a parameter space k_1 to k_5 is introduced in (8) to calibrate the total iron losses.

$$P_\mathrm{Fe} = k_1\, P_\mathrm{hyst} + k_2\, P_\mathrm{cl} + k_5\, P_\mathrm{exc} + k_{34} P_\mathrm{sat} \tag{8}$$

The parameter space represents the influence on the loss contributions due to manufacturing with respect to the standardized measurements resulting from SST or EF material characterizations. Consistently an optimal set of calibration factors should be found minimizing the error between calculated iron losses from standardized characterizations and machine measurements. The compensation factors can be derived by linear or nonlinear error minimization methods or by the semi-physical approach used here. Thus, the resulting optimal set of calibration factors and iron loss parameters can be determined. These resulting machine based iron loss parameters and the manufacturing influence can be compared to the conducted SST measurements except for eddy losses, as they are not influenced by cutting of a single lamination.

The determination of the machine based iron loss parameters presented here is derived from the semi-physical parameter identification. Hysteresis loss parameters are identified using quasi-static measurements, which is not possible in an application as a rotating electrical machine. Therefore, total losses are observed at slow speed to identify hysteresis and excess losses. There are two possibilities to identify excess and hysteresis losses. Analytically, using two different speeds and identification of the best parameter set at slow speed or low fundamental frequency. In the following, the analytic calculation of excess and hysteresis compensation factor is described.

As hysteresis losses scale linear with by frequency in (2), the excess parameter k_5 can be determined using two different measurements at slow speed. At low speed and at intermediate induction levels the saturation-loss contribution can be assumed to be negligible. The loss calculation in (8) scaled to the speed n can be written as follows in (9).

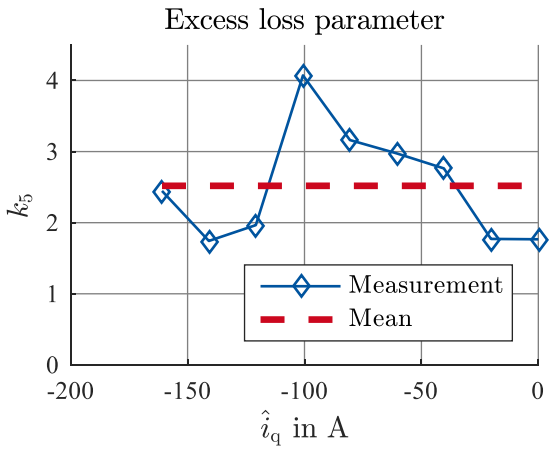

Fig. 4 Analytic identification of excess loss parameter $\boldsymbol{k_5}$ from test bench measurements.

$$\frac{k_1\, P_\mathrm{hyst}}{n} = \mathrm{const.} = \frac{(P_\mathrm{Fe}(n) - k_2\, P_\mathrm{cl}(n) - k_5\, P_\mathrm{exc}(n))}{n} \tag{9}$$

By using the measured iron losses P_Fe from the test bench at two different speed level, the calculated classical P_cl losses and the excess-loss contribution P_exc resulting from standardized measurements at the SST, the excess compensation factor k_5 can be determined by (10). The compensation factor represents the scaling factor between the machine measurements and the SST material characterization of 120 mm x 120 mm.

$$k_5 = \frac{\frac{(P_\mathrm{FE}(n_2) - P_\mathrm{cl}(n_2))}{n_2} - \frac{(P_\mathrm{FE}(n_1) - P_\mathrm{cl}(n_1))}{n_1}}{P_{exc}(n_2^{0.5} - n_1^{0.5})} \tag{10}$$

As demonstrated in (3) and (4) excess and classical eddy current losses are increased by higher harmonics. Even with short pitching and skewing the share of higher harmonics increase considerably with i_q. In case of the IPMSM, the magnetic design is rated to high induction levels even in no load case. Hence, the identification of parameter k_5 is done at pure direct current i_d. Fig. 4 demonstrates the resulting excess loss factor depending on direct current i_d and the resulting average value of k_5.

With fixed parameter k_5 the hysteresis loss parameter can be determined at slow speed. The hysteresis compensation factor k_1 results from minimizing the error ϵ between measured iron losses $P_\mathrm{Fe,meas}$ from the test bench, calculated classical P_{cl} and compensated excess loss contribution $P_\mathrm{exc} \cdot k_5$ summarized as $P_\mathrm{calc,komp.}$

$$\epsilon = \min\left\{\sum_{i=1}^{N}\sum_{j=1}^{N}\left(P_{\mathrm{Fe},meas}(i_{\mathrm{d},i}, i_{\mathrm{q},j}) - P_\mathrm{calc,komp.}(i_{\mathrm{d},i}, i_{\mathrm{q},j})\right)\right\} \tag{11}$$

The saturation losses are identified at high speed and current densities. The manufacturing process influences the resulting classical Foucault eddy current losses rather in terms of packaging and interlaminated short circuits than in terms of local cutting stress and strain. It is due to the fact that the parameters

determining the classical eddy current losses as the electrical conductivity and alloying content are not affected by cutting stress. However, the eddy-current calibration factor will be small as the influence is less pronounced. In a first step the linear calibration is performed, which can be extended to a nonlinear calibration in a second step.

III. Results

To derive an optimal iron loss parameter set from machine measurements using test bench measurements, this paper minimizes the overall losses including the iron loss comparable to a maximum energy control strategy. The resulting compensation factors consider the difference in iron loss calculation using standardized SST specimens of 120 mm x 120 mm and the resulting optimal losses parameters. The resulting machine based set of parameters can be compared to the adapted iron loss parameters considering the actual machine design.

Loss calculations of the machine simulation can be carried out considering higher harmonics n in (3) and (4) as done here or at the base frequency only. Fig. 5 demonstrates the measured total losses P_{Tot} at different speed ranges from (a) 250 min^{-1} to (d) 4000 min^{-1} dependent on the quadrature i_{q} and direct current i_{d}. Indicated with black contours are the calculated losses from standardized SST measurements and with red contours the calculated losses derived from machine measurements. It becomes apparent that with rising speed n and therefore rising fundamental frequency inside the iron core, calculated iron losses from ideal sinusoidal measurements diverge from machine test bench measurements. TABLE II lists exemplarily the calibration parameters $k_1 - k_5$ identified at different speed. For the identification of the model parameter the optimum is found for the absolute error. Thereby, the relative error in calculated losses at lower speeds can become bigger. An optimization on the relative error leads to an overrating of the small absolute share of iron losses at low speeds.

Hysteresis parameter k_1 identified at low speed clarifies the predicted strong increase in hysteresis losses due to manufacturing demonstrated in Fig. 3. Also excess loss parameter k_5 shows an significant increase of around in machine measurements compared to standardized characterization [19]. Saturation losses have a stronger frequency and flux density dependency and are exemplary identified at higher basic frequencies. Derived from the parameter identification of the iron loss formula, the saturation factor is determined at higher speed.

TABLE II. Calibration factors at different speeds

n in min^{-1}	k_1	k_2	k_{34}	k_5
250	1.68	1.0	1.0	2.08
1000	1.68	1.2	1.0	2.08
4000	1.68	1.2	2.0	2.08

At low speeds the identified hysteresis and excess current loss parameters, coping with the manufacturing influences describe the measured losses more accurately. At higher speeds of 3000 min^{-1} the impact of direct current i_{d} increases, resulting in an overestimation of calculated total iron losses for small values of i_{q}. Nevertheless, an improved loss prediction is achieved with machine based iron loss parameters compared to standardized SST or EF measurements.

A comparison between the adapted SST and machine based parameters is drawn in TABLE III. It is apparent that the adapted parameters of hysteresis and excess losses are in good accordance with resulting machine based calibration. In case of eddy current and higher harmonics the adapted parameters still underestimate the resulting measured losses. It is amongst other due to the fact of non-sinusoidal arbitrary wave forms inside the machines soft magnet material, which are not considered during standardized material characterization.

TABLE III. Comparison of resulting calibration factors, standard measurements and material parameters considering manufacturing influences.

	Std. (120mm)	Calibrated	Std. Adapted
a_1	$17.74 \cdot 10^{-3}$	$29.8 \cdot 10^{-3}$	$29.14 \cdot 10^{-3}$
α	2	-	1.61
a_2	$62.7 \cdot 10^{-6}$	$75.24 \cdot 10^{-6}$	-
a_3	0.11	2.7	0.23
a_5	$3.0 \cdot 10^{-4}$	$6.0 \cdot 10^{-4}$	$5.464 \cdot 10^{-4}$

IV. Conclusion

In this paper a methodology to derive machine based iron loss parameters using test bench measurements is presented. The methodology is derived from a semi-physical parameter identification of standardized material characterization. The Machine based iron losses at different speeds over the complete current density area are calibrated with respect to standardized single sheet measurements derived from SST measurements. The SST measurements are conducted considering manufacturing influences. This results in an adapted set of loss parameters, fine-tuned to the machine geometry.

A comparison of the compensation factors and loss parameters from standardized measurements, which result from specimen sizes considering the actual dimensions of the application is drawn. Machine based and resulting adapted parameters of hysteresis and excess losses are in good accordance. Higher harmonic saturation and eddy current losses still result in an underestimation due to the characterization under sinusoidal flux densities. The paper demonstrates the need of considering manufacturing influences in iron loss calculation. By linking standardized and machine measurements an a-priori assessment considering manufacturing influences is possible during design. In order to consider the manufacturing influence locally on both the flux density distribution and resulting iron losses local material models are necessary.

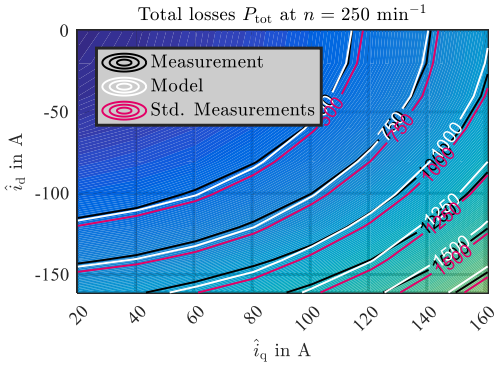

(a) Total losses at n = 250 min-1

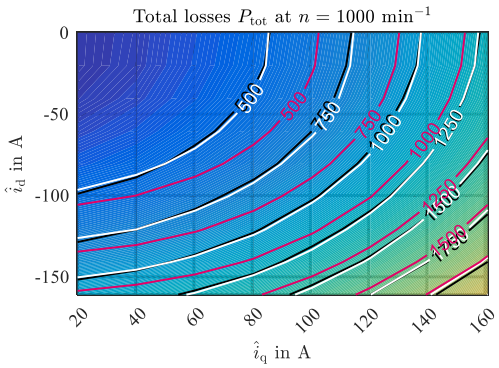

(b) Total losses at n = 1000 min-1

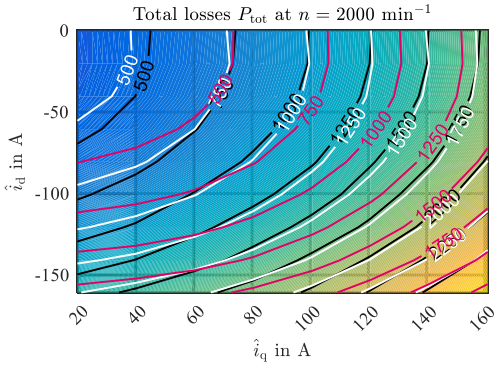

(c) Total losses at n = 2000 min-1

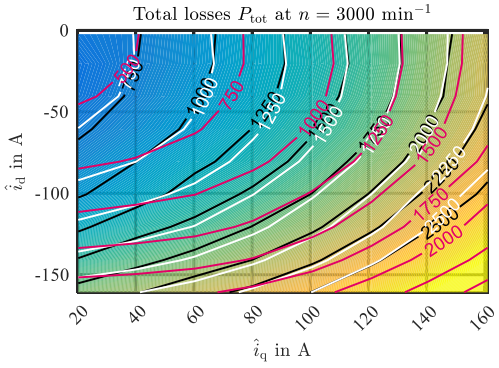

(d) Total losses at n = 3000 min-1

Fig. 5 (a) – (d) Comparison of measured (black contour) and resulting total losses using a ME control strategy with iron loss parameters from standardized single sheet measurements (red contour) and optimal parameter set derived from test bench measurements (white contour).

REFERENCES

[1] F. Fernandez-Bernal, A. Garcia-Cerrada, and R. Faure, "Determination of parameters in interior permanent-magnet synchronous motors with iron losses without torque measurement," *IEEE Trans. on Ind. Applicat,* vol. 37, no. 5, pp. 1265–1272, 2001.

[2] G.-x. Zhou, H.-j. Wang, D.-H. Lee, and J.-W. Ahn, "Study on efficiency optimizing of PMSM for pump applications," in *2007 7th Internatonal Conference on Power Electronics (ICPE)*, pp. 912–915.

[3] J. Lee, K. Nam, S. Choi, and S. Kwon, "A Lookup Table Based Loss Minimizing Control for FCEV Permanent Magnet Synchronous Motors," in *2007 IEEE Vehicle Power and Propulsion Conference (VPPC)*, pp. 175–179.

[4] R. Siebert, J. Schneider, and E. Beyer, "Laser Cutting and Mechanical Cutting of Electrical Steels and its Effect on the Magnetic Properties," *IEEE Trans. Magn,* vol. 50, no. 4, pp. 1–4, 2014.

[5] A. Schoppa, J. Schneider, and C.-D. Wuppermann, "Influence of the manufacturing process on the magnetic properties of non-oriented electrical steels," *Journal of Magnetism and Magnetic Materials*, vol. 215-216, pp. 74–78, 2000.

[6] S. Elfgen, S. Steentjes, S. Böhmer, D. Franck, and K. Hameyer, "Influences of material degradation due to laser cutting on the operating behaviour of PMSM using a continuous local material model," in *Electrical Machines ICEM 4-7 Sept. 2016*

[7] L. T. Mthombeni and P. Pillay, "Core Losses in Motor Laminations Exposed to High-Frequency or Nonsinusoidal Excitation," *IEEE Trans. on Ind. Applicat,* vol. 40, no. 5, pp. 1325–1332, 2004.

[8] B. Cougo, A. Tuysüz, J. Muhlethaler, and J. W. Kolar, "Increase of tape wound core losses due to interlamination short circuits and orthogonal flux components," in *IECON 2011: 37th annual conference of the IEEE Industrial Electronics Society ; Melbourne, Victoria, Australia, 7 - 10 November 2011,* Piscataway, NJ: IEEE, 2011, pp. 1372–1377.

[9] A. Schoppa, J. Schneider, C.-D. Wuppermann, and T. Bakon, "Influence of welding and sticking of laminations on the magnetic properties of non-oriented electrical steels," *Journal of Magnetism and Magnetic Materials*, vol. 254-255, pp. 367–369, 2003.

[10] S. Steentjes, M. Lessmann, and K. Hameyer, "Advanced iron-loss calculation as a basis for efficiency improvement of electrical machines in automotive application," in *2012 Electrical Systems for Aircraft, Railway and Ship Propulsion (ESARS)*, pp. 1–6.

[11] S. Elfgen, S. Steentjes, S. Böhmer, D. Franck, and K. Hameyer, "Continuous Local Material Model for Cut Edge Effects in Soft Magnetic Materials," *IEEE Trans. Magn,* vol. 52, no. 5, pp. 1–4, 2016.

[12] *Magnetic materials - Part 3: Methods of measurement of the magnetic properties of electrical steel strip and sheet by means of a single sheet tester*, IEC 60404-3:1992+A1:2002+A2:2009, 2010.

[13] S. Steentjes, M. Leßmann, and K. Hameyer, "Semi-physical parameter identification for an iron-loss formula allowing loss-separation," *J. Appl. Phys,* vol. 113, no. 17, 17A319, 2013.

[14] S. Jacobs, D. Hectors, F. Henrotte, M. Hafner, M. Herranz Gracia, K. Hameyer, and P. Goes, "Magnetic material optimization for hybrid vehicle PMSM drives," in *24th International Battery, Hybrid and Fuel Cell Electric Vehicle Symposium, EVS24*

[15] G. Bertotti, "Physical interpretation of eddy current losses in ferromagnetic materials. I. Theoretical considerations," *J. Appl. Phys,* vol. 57, no. 6, pp. 2110–2117, 1985.

[16] G. Bertotti, G. Di Schino, A. Ferro Milone, and F. Fiorillo, "On the effect of grain size on magnetic losses of 3% non-oriented SiFe," *J. Phys. Colloques*, vol. 46, no. C6, C6-385-C6-388, 1985.

[17] G. Bertotti, "General properties of power losses in soft ferromagnetic materials," *IEEE Trans. Magn,* vol. 24, no. 1, pp. 621–630, 1988.

[18] A. Ruf, A. Thul, S. Steentjes, and K. Hameyer, "Loss minimizing control strategy for electrical machines considering iron loss distribution," in *2015 IEEE International Electric Machines & Drives Conference (IEMDC)*, pp. 974–980.

[19] M. Hofmann, H. Naumoski, U. Herr, and H.-G. Herzog, "Magnetic Properties of Electrical Steel Sheets in Respect of Cutting: Micromagnetic Analysis and Macromagnetic Modeling," *IEEE Trans. Magn,* vol. 52, no. 2, pp. 1–14, 2016..